J Radioanal Nucl Chem (2011) 288:171–176
DOI 10.1007/s10967-010-0892-y

$^{99m}Tc(CO)_3$–Garenoxacin dithiocarbamate synthesis and biological evolution in rats infected with multiresistant *Staphylococcus aureus* and penicillin-resistant *Streptococci*

Syed Qaiser Shah · Aakif Ullah Khan · Muhammad Rafiullah Khan

Received: 12 October 2010 / Published online: 2 November 2010

Abstract $^{99m}Tc(CO)_3$–Garenoxacin dithiocarbamate ($^{99m}Tc(CO)_3$–GXND) complex was synthesized and biologically characterized in rats artificially infected with multiresistant *Staphylococcus aureus* (MDRSA) and penicillin-resistant *Streptococci* (PRSC). The characteristics of the $^{99m}Tc(CO)_3$–GXND complex was assessed in terms of radiochemical stability in saline, serum, in vitro binding with live and heat killed MDRSA and PRSC and biodistribution in rats artificially infected with MDRSA and PRSC. The complex showed maximum radiochemical stability at 30 min and remained more than 90% stable up to 240 min in normal saline after reconstitution. The complex was found stable in serum at 37 °C up to 16 h. The complex showed in vitro saturated binding with living MDRSA and PRSC. In rats infected with living MDRSA and PRSC the complex showed five higher up take in the infected muscle as compared to the inflamed and normal muscle. No significant difference in uptake of the complex in rats infected with heat killed MDRSA and PRSC was observed. The disappearance of the complex from the blood and appearance in the urinary system confirm the normal biological route of biodistribution and excretion. The high values of the radiochemical stability in normal saline, serum, saturated in vitro binding with living MDRSA and PRSC and significant infected to normal muscles ratios, the $^{99m}Tc(CO)_3$–GXND complex is recommended for the localization of soft tissue infection caused by living MDRSA and PRSC.

Keywords Garenoxacin dithiocarbamate · $^{99m}Tc(CO)_3$–GXND complex · MDRSA · PRSC

S. Q. Shah (✉)
Nuclear Medicine Research Laboratory (NMRL), University of Peshawar, Peshawar, KPK, Pakistan
e-mail: ssqaiser2002@yahoo.com

A. U. Khan
Nuclear Medicine, Oncology and Radiotherapy Institute (NORI), Islamabad, Pakistan

M. R. Khan
Phytopharmaceutical & Neutraceuticals Research Laboratory (PNRL), University of Peshawar, Peshawar, KPK, Pakistan

Introduction

The role of bacterial infection in the existing high rate of morbidity and mortality is very vital and still a serious concern of the clinician for its early diagnosis and timely management with appropriate drug. The role of the modern analytical techniques like ultrasonography, computed tomography and magnetic resonance imaging are unsatisfactory in diagnosis of infection and its discrimination from inflammation [1–3].

The Nuclear Medicine Gamma Scintigraphy has proven a specific and accurate tool for the early diagnosis of the deep soft tissue in vivo infection after the introduction of γ-emitting technetium-99m (^{99m}Tc) labeled radiopharmaceuticals [4–16]. Our recently reported infection imaging radiopharmaceuticals [17–22] that shown promising results in detection of different infection caused by different pathogens, sustained our effort and encouraged us to develop more specific and promising radiopharmaceutical.

The ciprofloxacin and ofloxacin are the fluoroquinolones having broad spectrum antibiotic activity against a wide range of pathogens and it is believed that for the antibiotic activity of the fluoroquinolones the presence of fluorine at position C-6 in the quinolones skeleton is obligatory. Garenoxacin (GXN) (Fig. 1) is a newly developed quinolone showing exceptional antibiotic activity against Gram

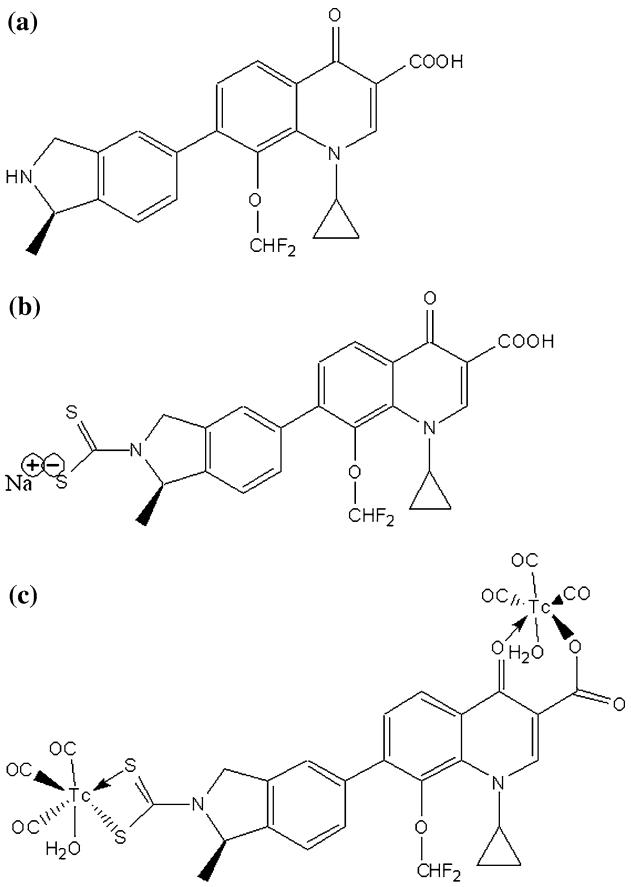

Fig. 1 **a** Chemical structure of GXN. **b** GXND. **c** Proposed structure of the $^{99m}Tc(CO)_3$–GXND complex

positive and Gram negative bacteria including methicillin-resistant *Staphylococci* (MDRSA) and penicillin-resistant *Streptococci* (PRSC) [23, 24].

In extension to our continuing investigation owing to the current needs, now we report an efficient radiolabeling method of Garenoxacin dithiocarbamate (GXND) with the γ-emitting ^{99m}Tc using the $[^{99m}Tc(CO)_3(H_2O)_3]^+$ as the staring material. In the current investigation the $^{99m}Tc(CO)_3$–GXND complex was characterized in terms of radiochemical stability in saline, in vitro stability in serum, in vitro binding with living and heat killed MDRSA and PRSC and biodistribution in artificially living MDRSA and PRSC infected rats.

Experimental

Materials

Garenoxacin (Bristol-Myers Squibb, Syracuse, UK), TLC (Merck) and all the other chemicals and solvents of analytical grade (Sigma). RP-HPLC (Shimadzu, Japan) well counter and scalar count rate meter (Ludlum, USA) Dose calibrator (Capintech, USA) and Gamma camera GKS-1000 (GEADE Nuclearmedizine system, Germany).

Method

Preparation of GXND and its ^{99m}Tc-tricarbonyl complexation

Garenoxacin dithocarbamate was synthesized using the reported method [22] and thereafter its labeling with ^{99m}Tc was assessed using $[^{99m}Tc(OH_2)_3(CO)_3]^+$ precursor by adding 0.5 mL (1–2 mCi) of sodium pertechnetate ($Na^{99m}TcO_4^-$,) through a sterilized insulin syringe to the kit (Isolink) and for 15 min incubated with 0.1 mol/mL HCl solution. Thereafter, 1–5 mg (with 1 mg increment) dissolved in water was added to the reaction mixture through insulin syringe and incubated at room temperature for 15 min.

Determination of partition coefficient

Partition coefficient of the ^{99m}Tc-tricarbonyl complex of GXND was determined using the reported method [22]. Briefly, mixture of the $^{99m}Tc(CO)_3$–GXND radiocomplex, octanol and phosphate buffer in equivalent volume was vortexed for 5 min at room temperature followed by centrifugation at 5,000 rpm/min for 15 min. Thereafter, 0.1 mL aliquot was drawn at different times and counted for activity using well counter interface with scalar count rate meter. Using the following formula partition coefficient was calculated.

$$P = \frac{(\text{Counts per min in octanol} - \text{counts per min in background})}{(\text{Counts per min in buffer} - \text{counts per min in background})}$$

Determination of radiochemical purity of the $^{99m}Tc(CO)_3$–GXND complex

Radiochemical purity (RCP) yield of the $^{99m}Tc(CO)_3$–GXND radiocomplex in normal saline was determined using Shimadzu HPLC (SCL-10 AVP) system equipped with UV (SDP-10 AVP) detector working at 254 nm, flow scintillation (packard 500 TR series) analyzer, binary pump, and online degasser. Aliquots, 10 µL of the $^{99m}Tc(CO)_3$–GXND complex were injected to the main unit of the HPLC. C-18 column (4.6 × 150 mm) was used as a stationary phase and water :methanol was used as a mobile phase. A flow rate of 1 mL/min was maintained for 15 min using different combinations of the mobile phase. (0–3 min (100:00), 3–5 min (60:40), 5–8 min (55:45), 8–10 (25:75), 10–13 (00:100) and 13–15 (100:100)). The fractions collected during 1–15 min of elution were counted individually for activity using the single gamma rays detecting well

counter interface with scalar count rate meter. The RCP yield of the ^{99m}Tc(CO)$_3$–GXND complex was compared with the ^{99m}TcN–GXND complex.

Serum stability

^{99m}Tc(CO)$_3$–GXND radiocomplex was assessed for its in vitro stability at different intervals in the serum using thin layer chromatography. 0.2 mL of the ^{99m}Tc(CO)$_3$–GXND radiocomplex was incubated at 37 °C with 1.8 mL of serum. Subsequently, at 2, 4, 6, 8, 10, 12, 14 and 16 h of incubation aliquots were spotted on the polyamide strip. Thereafter, the strips were developed in saline and CH_2Cl_2: CH_3OH (9:1) (v/v) and counted for activity using single well gamma rays detecting well counter interface with scalar count rate meter. The in vitro stability values of the ^{99m}Tc(CO)$_3$–GXND in serum was compared with the ^{99m}TcN–GXND radiocomplex.

Bacterial binding

The binding of MDRSA and PRSC of the ^{99m}Tc(CO)$_3$–GXND radiocomplex was investigated using the reported method [25]. Briefly, 10 MBq of the freshly prepared ^{99m}Tc(CO)$_3$–GXND radiocomplex was decanted into a sterilized test tube containing 0.1 mL sodium phosphate buffer (Na-PB). Thereafter, 0.8 mL (50%, v/v) 0.01 M acetic acid containing approximately 1×10^8 colony forming units (CFU) of MDRSA was added followed by incubation at 4 °C for 1 h with a final pH 5. The blend was centrifuged for 10 min (2,000 rpm) followed by removal of the supernatant. The pellets were resuspended in Na-PB (2 mL) and re-centrifuged for 10 min with the same spin speed. For the estimation of the bacterial binding the pellets were counted for % uptake using single well gamma rays detecting counter attached with scalar count rate meter. The same process was repeated for the PRSC.

Biodistribution

The in vivo of the ^{99m}Tc(CO)$_3$–GXND radiocomplex was investigated in artificially infected male Sprague–Dawley rats (weight, 180–220 g). Randomly, sixteen healthy rats were selected and separated into four groups (**A, B, C** and **D**) with four rats in each group. All the rats were intramuscularly (IM) injected with 0.2 mL autoclaved sterile turpentine oil into the left thigh. 0.2 mL containing approximately 1×10^8 CFU of live MDRSA was IM injected to the right thigh of the group **A** rats and a similar amount of heat killed MDRSA to the group **B**. Similarly, 0.2 mL of live PRSC was IM injected to the right thigh of the group **C** and a similar amount of heat killed PRSC to the group **D**. After 24 h, 0.5 mL (18.5 MBq) of the ^{99m}Tc(CO)$_3$–GXND radiocomplex was intravenously (I.V.) injected to all the rats and then executed in accordance with the rules and regulations of the Nuclear Medicine Research Laboratory (NMRL), University of Peshawar. For each of the rats the percent absorbed dose of the injected ^{99m}Tc(CO)$_3$–GXND radiocomplex per gram in blood, liver, spleen, stomach, intestine, kidney, infected muscle, inflamed and normal muscle was calculated using single well gamma rays detecting counter attached with scalar count rate meter.

Result and discussion

Radiochemistry of the ^{99m}Tc(CO)$_3$–GXND complex

Garenoxacin (Fig. 1a) was converted to its dithiocarbamate derivative (GXND) (Fig. 1b) and radiolabeled with ^{99m}Tc using the $[^{99m}Tc(CO)_3(H_2O)_3]^+$ precursor as the staring material to give ^{99m}Tc(CO)$_3$–GXND radiocomplex as shown in Fig. 1c. In the *fac*-$[^{99m}Tc(CO)_3(H_2O)_3]^+$ originator the GXND eagerly displaced water to give the ^{99m}Tc(CO)$_3$–GXD complex. The proposed structure of the ^{99m}Tc(CO)$_3$–GXND radiocomplex will have a square planner bipyramidal geometry with ^{99m}Tc(CO)$_3$:ligand ratio of 2:1 [26].

Lipophilicity of the ^{99m}Tc(CO)$_3$–GXND radiocomplex

A decrease in the values of the participation coefficient was observed for the ^{99m}Tc(CO)$_3$–GXND radiocomplex. The *P* value calculated for ^{99m}Tc(CO)$_3$–GXND and ^{99m}TcN–GXND radiocomplexes were 0.44 ± 0.01 and 1.08 ± 0.02, respectively. The *P* values of both the radiocomplexes suggested that both are lipophilic.

RP-HPLC characterization of the ^{99m}Tc(CO)$_3$–GXND radiocomplex

The HPLC chromatogram of the ^{99m}Tc(CO)$_3$–GXND radiocomplex as given in Fig. 2 showed distinctly two variable peaks with a retention time (RT) of 3.3 and 11.7 min. The peak at 11.7 represents the yield of the ^{99m}Tc(CO)$_3$–GXND radiocomplex. The GXND radiocomplex prepared through $[^{99m}TcN]^{2+}$ core also showed similar HPLC profile with slightly different RT. The two peaks at RT 4.4 and 12.6 min was observed for the ^{99m}TcN–GXND radiocomplex. The peak observed at RT 12.6 min represents the ^{99m}TcN–GXND radiocomplex.

In normal saline, at different intervals after reconstitution the ^{99m}TcN–GXND radiocomplex showed stable in vitro radiochemical purity yield as given in Fig. 3. The RCP values of the ^{99m}TcN–GXND radiocomplex calculated at

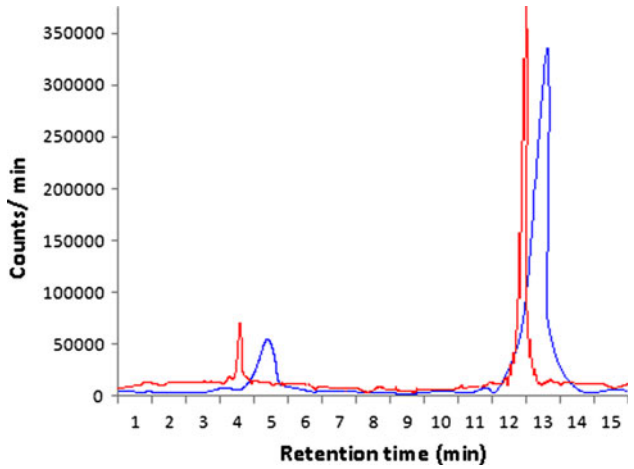

Fig. 2 HPLC chromatogram of the of the $^{99m}Tc(CO)_3$–GXND complex (*Red* trace represents $^{99m}Tc(CO)_3$–GXND and *blue* ^{99m}TcN–GXND complex)

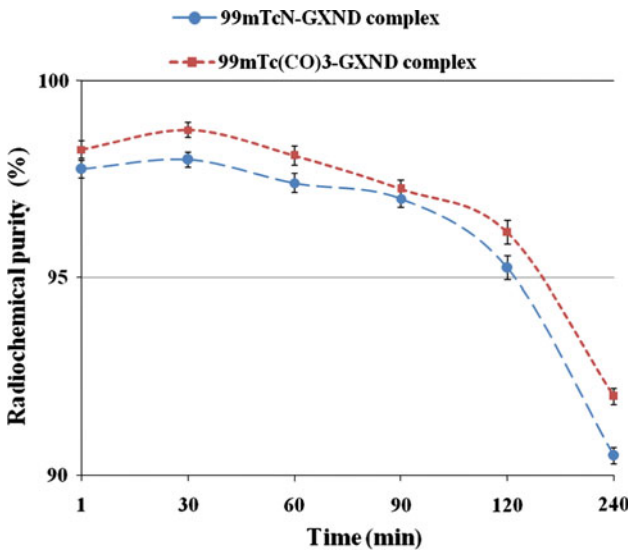

Fig. 3 Radiochemical purity of the $^{99m}Tc(CO)_3$–GXND and ^{99m}TcN–GXND complexes in saline

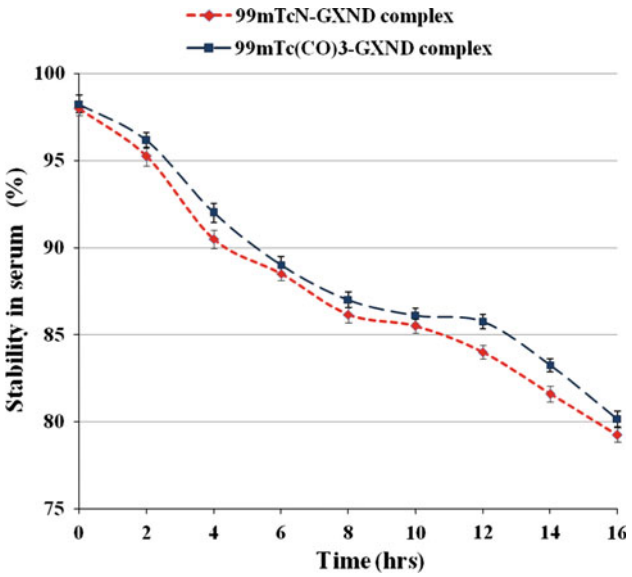

Fig. 4 In vitro stability of the $^{99m}Tc(CO)_3$–GXND and ^{99m}TcN–GXND complex in serum

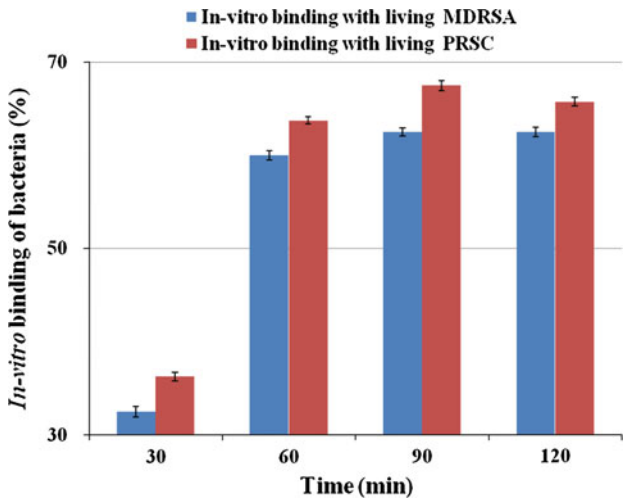

Fig. 5 In vitro binding of $^{99m}Tc(CO)_3$–GXND complex with living MDRSA and PRSC at different intervals at 37 °C

different intervals decreases with time. After 30 min of the reconstitution 98.25 ± 0.22% RCP yield was observed. The RCP yield decreased with in 4 h by 6.75–92.00%. The RCP yield of the $^{99m}Tc(CO)_3$–GXND was found insignificantly higher than the ^{99m}TcN–GXND radiocomplexes. No significant difference was observed between the RCP yields of the both the complexes even after 4 h of reconstitution.

Stability of the $^{99m}Tc(CO)_3$–GXND radiocomplex in serum

The in vitro stability of the $^{99m}Tc(CO)_3$–GXND radiocomplex in serum at 37 °C (up to 16 h) is given in Fig. 4. The complex showed stable in vitro behavior in serum at 37 °C up to 4 h. The stability insignificantly went down to 81.50 ± 0.45% after 16 h.

MDRSA and PRSC bacterial uptake

Both the live colonies of the pathogens (MDRSA and PRSC) showed a similar saturated but slightly different uptake as given in Fig. 5. The uptake affinity of the MDRSA is slightly higher than PRSC. However, insignificantly low binding was observed in both the heat killed MDRSA and PRSC.

Table 1 Distribution of ^{99m}TcN–GXND and ^{99m}Tc(CO)3–GXND complexes in various organs of rats artificially infected with living MDRSA

Organs/tissues (g)	Percent in vivo distribution							
	^{99m}TcN–GXND at different intervals (in min)				^{99m}Tc(CO)$_3$–GXND at different intervals (in min)			
	30	60	90	120	30	60	90	120
Infected muscle	6.00 ± 0.24	12.75 ± 0.22	13.90 ± 0.22	13.50 ± 0.21	6.50 ± 0.20	12.00 ± 0.24	12.50 ± 0.19	11.00 ± 0.22
Inflamed muscle	3.50 ± 0.22	3.50 ± 0.24	3.00 ± 0.20	3.00 ± 0.22	3.00 ± 0.24	3.25 ± 0.20	3.50 ± 0.24	3.15 ± 0.21
Normal muscle	3.00 ± 0.24	2.50 ± 0.22	2.50 ± 0.20	2.50 ± 0.21	3.25 ± 0.20	3.00 ± 0.21	2.50 ± 0.24	2.50 ± 0.22
Blood	22.50 ± 0.22	8.50 ± 0.21	7.00 ± 0.20	3.50 ± 0.24	22.00 ± 0.20	9.25 ± 0.24	7.55 ± 0.22	4.00 ± 0.19
Liver	18.75 ± 0.22	13.00 ± 0.24	9.10 ± 0.21	5.10 ± 0.24	16.50 ± 0.22	10.00 ± 0.20	8.75 ± 0.24	4.75 ± 0.20
Spleen	8.55 ± 0.24	7.00 ± 0.21	5.00 ± 0.22	3.00 ± 0.20	9.00 ± 0.21	7.50 ± 0.24	6.25 ± 0.20	4.00 ± 0.24
Kidney	9.50 ± 0.22	18.50 ± 0.24	21.55 ± 0.22	24.00 ± 0.23	9.00 ± 0.20	20.50 ± 0.22	22.00 ± 0.24	23.45 ± 0.20
Stomach & intestines	8.55 ± 0.20	7.00 ± 0.22	5.75 ± 0.24	3.00 ± 0.21	8.00 ± 0.19	7.25 ± 0.20	5.50 ± 0.22	3.25 ± 0.24

Table 2 Distribution of ^{99m}TcN–GXND and ^{99m}Tc(CO)$_3$–GXND complexes in various organs of rats artificially infected with living PRSC

Organs/tissues (g)	Percent in vivo distribution							
	^{99m}TcN–GXND at different intervals (in min)				^{99m}Tc(CO)$_3$–GXND at different intervals (in min)			
	30	60	90	120	30	60	90	120
Infected muscle	7.50 ± 0.20	13.25 ± 0.24	14.00 ± 0.20	13.75 ± 0.20	7.25 ± 0.22	12.75 ± 0.20	13.50 ± 0.24	13.15 ± 0.24
Inflamed muscle	4.00 ± 0.24	3.50 ± 0.20	3.00 ± 0.21	3.00 ± 0.19	4.50 ± 0.20	4.00 ± 0.22	3.25 ± 0.24	3.00 ± 0.22
Normal muscle	3.50 ± 0.20	3.00 ± 0.24	2.50 ± 0.22	2.50 ± 0.20	3.00 ± 0.24	3.50 ± 0.20	2.75 ± 0.22	2.50 ± 0.24
Blood	18.75 ± 0.24	10.00 ± 0.21	8.25 ± 0.24	4.25 ± 0.20	16.50 ± 0.24	11.25 ± 0.22	9.00 ± 0.20	4.55 ± 0.19
Liver	16.50 ± 0.20	12.75 ± 0.20	7.55 ± 0.24	4.85 ± 0.20	17.25 ± 0.20	10.45 ± 0.24	6.75 ± 0.20	4.50 ± 0.24
Spleen	7.25 ± 0.24	6.00 ± 0.24	4.55 ± 0.20	3.50 ± 0.22	6.50 ± 0.19	5.75 ± 0.22	4.00 ± 0.24	3.25 ± 0.20
Kidney	10.00 ± 0.21	17.75 ± 0.20	20.15 ± 0.24	22.50 ± 0.20	12.50 ± 0.24	18.15 ± 0.22	22.00 ± 0.20	23.50 ± 0.19
Stomach & intestines	7.50 ± 0.24	6.10 ± 0.22	5.25 ± 0.20	3.50 ± 0.20	8.25 ± 0.20	7.50 ± 0.20	6.00 ± 0.19	4.15 ± 0.24

Biodistribution

The percent absorbed dose of the injected ^{99m}Tc(CO)$_3$–GXND radiocomplex per gram in blood, liver, spleen, stomach, intestine, kidney, infected muscle, inflamed and normal muscle of the rats of group **A** and **B** is given in Table 1 and of group **C** and **D** in Table 2. Initially high level of the ^{99m}Tc(CO)$_3$–GXND radiocomplex was found per gram of the blood in the all groups. However, a significant decline was observed with time in all the rats infected with living or heat killed MDRSA and PRSC. In rats infected with living MDRSA (group **A**) and PRSC (group **C**) significantly higher activity of the ^{99m}Tc(CO)$_3$–GXND radiocomplex was observed in infected muscle as compared to inflamed and normal muscle. However, in rats infected with heat killed MDRSA (group **B**) and PRSC (group **C**) no significant difference in the level of activity of the ^{99m}Tc(CO)$_3$–GXND radiocomplex was observed in infected, inflamed and normal muscle. The level of activity of the ^{99m}Tc(CO)$_3$–GXND radiocomplex initially in the liver and spleen was high and lower in the kidney in all the groups. However the level of activity went down in liver and spleen and went up in kidneys and urine irrespective of the living or heat killed

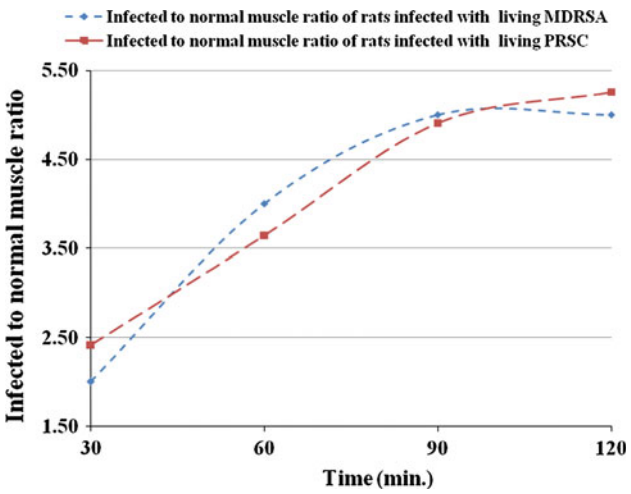

Fig. 6 Infected to normal muscle ratio of the ^{99m}Tc(CO)$_3$–GXND in rats infected with living MDRSA and PRSC

MDRSA or PRSC induced infection. The appearance of activity of the $^{99m}Tc(CO)_3$–GXND radiocomplex in urinary system and disappearance from circulatory system confirmed the normal route of excretion.

Figure 6 gives the ratio of the $^{99m}Tc(CO)_3$–GXND radiocomplex uptake in MDRSA and PRSC infected rats. Similar uptake ratio was observed in group **A** and **C** rats. The level of activity uptake in infected muscle, in both the groups of the rats infected with living pathogens, were significantly higher than in inflamed and normal muscle.

Conclusion

Radiocomplexation of the GXND with ^{99m}Tc using $[^{99m}Tc(OH_2)_3(CO)_3]^+$ precursor was assessed and biologically investigated as potential MDRSA and PRSC infection radiotracer. The results of the radiochemical stability in saline, serum, in vitro MDRSA and PRSC uptake, percent absorbed dose per gram in blood, liver, spleen, stomach, intestine, kidney, infected muscle, inflamed and normal muscle and infected to inflamed and normal muscle ratio confirmed the suitability of the $^{99m}Tc(CO)_3$–GXND radiocomplex as potential MDRSA and PRSC in vivo infection radiotracer.

References

1. Gallagher H, Ramsay SC, Barnes J, Maggs J, Cassidy N, Ketheesan N (2006) Neutrophil labeling with [^{99m}Tc]-technetium stannous colloid is complement receptor 3-mediated and increases the neutrophil priming response to lipopolysaccharide. Nucl Med Biol 33:433
2. Basu S, Chryssikos T, Moghadam-Kia S, Zhuang H, Torigian DA, Alvai A (2009) Positron emission tomography as a diagnostic tool in infection: present role and future possibilities. Semin Nucl Med 39:36
3. Lahiri S, Sarkar S (2007) Studies on 66, 67Ga– and 199Tl–poly(*N*-vinylpyrrolidone) complexes. Appl Radiat Isot 65:309
4. Chattopadhyay S, Das SS, Chandra S, De K, Mishra M, Sarkar BR, Sinha S, Ganguly S (2010) Synthesis and evaluation of ^{99m}Tc–moxifloxacin, a potential infection specific imaging agent. Appl Radiat Isot 68:314
5. Motaleb MA (2007) Preparation of ^{99m}Tc–cefoperazone complex, a novel agent for detecting sites of infection. J Radioanal Nucl Chem 272:167
6. Motaleb MA (2007) Preparation and biodistribution of ^{99m}Tc–lomefloxacin and ^{99m}Tc–olfloxacin complex. J Radioanal Nucl Chem 272:95
7. Zhang J, Guo H, Zhang S, Lin Y, Wang X (2008) Synthesis and biodistribution of a novel ^{99m}TcN complex of ciprofloxacin dithiocarbamate as a potential agent for infection imaging. Bioorg Med Chem Lett 18:51
8. Roohi S, Mushtaq A, Jehangir M, Ashfaq MS (2006) Synthesis, quality control and biodistribution of ^{99m}Tc–Kanamycin. J Radioanal Nucl Chem 267:561
9. Oh SJ, Ryu J, Shin JW, Yoon EJ, Ha H, Cheon JH, Lee HK (2002) Synthesis of ^{99m}Tc–ciprofloxacin by different methods and its biodistribution. Appl Radiat Isot 57:193
10. EL-Gany EA, EL-Kolaly MT, Amine AM, EL-Sayed AS, Abdel-Gelil F (2005) Synthesis of ^{99m}Tc–pefloxacin: a new targeting agent for infectious foci. J Radioanal Nucl Chem 266:131
11. Motaleb MA (2009) Preparation, quality control and stability of ^{99m}Tc–sparafloxacin complex, a novel agent for detecting sites of infection. J Label Compd Radiopharm 52:415
12. Xia J, Wang Y, Yu J, Li S, Tang L, Zheng M, Liu X, Li G, Cheng D, Liang S, Yin D (2008) Synthesis, in vitro and in vivo behavior of ^{188}Re(I)–tricarbonyl complexes for the future functionalization of biomolecules. J Radioanal Nucl Chem 275:325
13. Zhang J, Wang X, Jin C (2007) Synthesis and biodistribution of the $^{99m}Tc(CO)_3$–DEDT complex as a potential new radiopharmaceutical for brain imaging. J Radioanal Nucl Chem 272:91
14. Djokic DD, Jankovic DL, Stamenkovic LL, Pirmettis I (2004) Chemical and biological evaluation of $^{99m}Tc(CO)_3$ and ^{99m}Tc complexes of some IDA derivatives. J Radioanal Nucl Chem 260:471
15. Xia J, Long S, Yu J, Wang Y, Cao Z (2009) Pyridyl derivatives provide new pathways for labeling protein with *fac*-$[^{188}Re(CO)_3(H_2O)_3]^+$. J Radioanal Nucl Chem 281:493
16. Zhang JB, Wang XB, Jin C (2006) Synthesis of $^{99m}Tc(CO)_3$–NOET via $[^{99m}Tc(OH_2)_3(CO)_3]^+$ precursor and comparative biological studies with ^{99m}TcN–NOET. J Radioanal Nucl Chem 269:227
17. Qaiser SS, Khan AU, Khan MR (2010) Synthesis, biodistribution and evaluation of ^{99m}Tc–Sitafloxacin kit: a novel infection imaging agent. J Radioanal Nucl Chem 284:189
18. Shah SQ, Khan AU, Khan MR (2010) Radiosynthesis of ^{99m}Tc–nitrifuratonin a novel radiotracer for in vivo imaging of *Escherichia coli* infection. J Radioanal Nucl Chem. doi:10.1007/s10967-010-0697-z
19. Shah SQ, Khan AU, Khan MR (2010) Radiosynthesis and biodistribution of ^{99m}Tc–rifampicin: a novel radiotracer for in vivo infection imaging. Appl Radiat Isot 68:2255
20. Shah SQ, Khan AU, Khan MR (2010) ^{99m}Tc–Novobiocin: a novel radiotracer for infection imaging. Radiochim Acta (in press)
21. Shah SQ, Khan AU, Khan MR (2010) Radiosynthesis, biodistribution and scintigraphy of the ^{99m}Tc–Teicoplanin complex in artificially infected animal models. J Label Compd Radiopharm (in press)
22. Shah SQ, Khan AU, Khan MR (2010) Radiosynthesis and biological evaluation of ^{99m}Tc–sitafloxacin dithiocarbamate as potential radiotracer for *Staphylococcus aureus* infection. J Radioanal Nucl Chem. doi:10.1007/s10967-010-833-9
23. Sader HS, Fritsche TR, Jones RN (2007) In vitro activity of garenoxacin tested against a worldwide collection of ciprofloxacin-susceptible and ciprofloxacin-resistant Enterobacteriaceae strains (1999–2004). Diagn Microbiol Infect Dis 58:27
24. Roblin PM, Reznik T, Hammerschlag MR (2003) In vitro activity of garenoxacin against recent clinical isolates of *Chlamydia pneumoniae*. Int J Antimicrob Agents 21:578
25. Welling MM, Paulusma-Annema A, Batler HS, Pauwels EKJ, Nibbering PH (2000) Technetium-99m labelled antimicrobial peptides discriminate between bacterial infections and sterile inflammations. Eur J Nucl Med 27:292
26. Baldas J, Bonnyman J, Poer PM, Williams GA, Mackay MF (1981) Synthesis and structure of bis(diethyldithiocarbamato)nitridotechnetium(V)—a technetium-nitrogen triple bond. J Chem Soc Dalton Trans 9:1798